

18 μm electrodeposited copper foil for flex fatigue applications

Harish D. Merchant

Gould Electronics, Eastlake, Ohio, USA

Melvin G. Minor Jr

Gould Electronics, Eastlake, Ohio, USA

Sid J. Clouser

Gould Electronics, Eastlake, Ohio, USA

Dan T. Leonard

Gould Electronics, Eastlake, Ohio, USA

Keywords

Copper, Fatigue, Flexible circuit, Strain

Abstract

The strain-based flex fatigue of 18 μm thick copper foil is evaluated over a wide range of strain amplitudes. Seven electrodeposited foils, four commercial grades and three experimental foils, and a commercial grade rolled foil are characterized. The fatigue life versus cyclic strain amplitude curve in the high strain amplitude (low cycle) and low strain amplitude (high cycle) regimes is developed for each foil. On the basis of fatigue life (N_f) and fatigue ductility (D_f), the low cycle fatigue performance of eight foils is ranked. Universal correlations of N_f and D_f with the uniaxial tensile strength are established. Two electrodeposited foils, experimental foil DF 8 in the high strain amplitude regime and commercial foil DF 9 in the low strain amplitude regime, have been shown to display fatigue performance comparable to that of the commercial rolled GR 8 foil.

Introduction

The flexible circuit is often subjected to repetitive reversible strain due to mechanical motion of the circuit (or due to the ambient temperature fluctuations). The cumulative effect of strain cycling, that is fatigue, is to damage the copper conductor line and hence to impact its electrical function. The number of cycles to failure, the fatigue life (N_f), corresponds to the associated fatigue damage and depends inversely upon the strain amplitude per cycle ($\Delta\epsilon/2$). High $\Delta\epsilon/2$ induces plastic deformation of copper and the failure occurs after relatively small N_f (low cycle fatigue); low $\Delta\epsilon/2$ induces an overall elastic deformation of copper and the failure occurs after a large N_f (high cycle fatigue).

Generally, both the elastic ($\Delta\epsilon_e$) and plastic ($\Delta\epsilon_p$) components of strain are present during fatigue such that (Dowling, 1993) $\Delta\mu = \Delta\epsilon_p + \Delta\epsilon_e$. The fatigue life is related to the strain amplitude by power relationship. Coffin-Manson relation (Courtney, 1990):

$$\frac{\Delta\epsilon}{2} = \epsilon_f' (2N_f)^c + \frac{\sigma_f'}{E} (2N_f)^b \quad (1)$$

where $2N_f$ is the number of strain reversals, E is Young's modulus, ϵ_f' is related to ductility and σ_f' to strength of copper in cyclic loading, and exponents b and c are negative. The first term is predominant during the low cycle fatigue, the second term is predominant during the high cycle fatigue and both terms are contributory during the transition from the plastic to elastic response of copper; the transition fatigue life, N_t , is given by equating the two terms:

$$N_t = \frac{1}{2} \frac{(\sigma_f')^{(c-b)^{-1}}}{(E\epsilon_f')} \quad (2)$$

For most metals, $c = -0.5$, $b = -0.1$ and $N_t \approx 10^4$.

We have investigated the flex fatigue of seven 18 μm thick electrodeposited copper foils, four commercial grades and three experimental foils, in the low cycle and high cycle fatigue regimes, employing a wide range of $\Delta\epsilon/2$ between 3×10^{-4} and 3×10^{-2} (0.03 and 3 per cent) for N_f between 40 and 3.5×10^6 . For comparison, 18 μm thick commercial (ETP copper) rolled foil has been characterized under identical conditions. The results are fitted to equation (1) and for each foil we have established:

- 1 ranges of low cycle and high cycle fatigue;
- 2 N_t as defined by equation (2);
- 3 fatigue directionality (longitudinal versus transverse); and
- 4 effect of annealing.

The Coffin-Manson plots are carefully analyzed, compared and ranked in terms of fatigue life N_f and fatigue ductility D_f (Englemaier, 1987).

Experimental procedure

The flex fatigue tests were performed as per the ASTM E286a and E 345 guidelines. The 18 μm commercial grade electrodeposited foils GR 1, GR 2, GR 3 and DF 9 and the

experimental electrodeposited foils DF 8, EF and TCAM were characterized. For comparison, the 18 μm commercial grade (ETP copper) rolled foil GR 8 was also tested. The test coupons were cut in the longitudinal and transverse orientations with respect to the foil surface roll markings, prior to (as-fabricated) and following (annealed) a 225°C, ten minutes anneal (to simulate the substrate and coverlay lamination thermal exposures).

The fatigue tests were conducted at 1 Hz with 84g stretch load, which corresponds to 2,000 psi stress (much less than the pre-anneal or post-anneal yield or ultimate strength of the foil), to conform to the mandrel radius of curvature during cyclic flexing. The mandrel diameters between 31 and 750 mil (0.775 and 18.75mm) were utilized to provide a range of strain amplitudes $\Delta\epsilon/2$ between 3×10^{-2} and 6×10^{-4} (3 and 0.06 per cent); as per the relation $\Delta\epsilon/2 = t_m / (2p + t)$ where t_m is the mean core thickness and t the micrometer thickness of the foil ($t - t_m$ is the average foil surface profile) and $2p$ is the mandrel diameter.

For the low cycle fatigue, each data point represents an average of three N_f readings; the scatter between readings was generally less than 10 per cent. For the high cycle fatigue, N_f (hence the time to obtain a reading) and the scatter between readings increased with the mandrel diameter. In this regime, an average of two readings represents a data point.

Results

(i) Low cycle fatigue

Figures 1-3 show the high amplitude, low cycle fatigue Coffin-Manson plots on a logarithmic scale. Figures 1 and 2 for the commercial foils and Figure 3 for the experimental foils. The data are shown beyond $2N_f = 10^4$ in order to delineate the "knee" for the plastic to elastic transition. Note that the longitudinal versus transverse anisotropy is small for the experimental EF and DF 8 foils and relatively large for the GR 8 (rolled) and TCAM foils. The non-parallel directional curves for the GR 8 foil are apparently related to its pancaked grain structure (Merchant *et al.*, 1996).

The transition fatigue life N_t (equation 2) is generally around 10^4 ; the annealing increases N_t somewhat. A glaring exception is the transversely oriented GR 8 foil where upon annealing the anneal induced embrittlement (Merchant and Clouser, 1996) causes N_t to shift from above 10^4 to below 10^3 . The fatigue damage in the as-fabricated transversely oriented GR 8 foil has been shown to occur by tearing along the boundaries of the pancaked grains (Merchant *et al.*, 1996).

The parameters c and ϵ_f' in equation (1) are determined from the average low cycle fatigue plot: the slope represents c and the intercept at $2N_f = 1$ (half strain cycle or one strain reversal) on the strain amplitude axis represents ϵ_f' . Typical values for the GR 8 foil in the longitudinal orientation are $c = -0.46$, $\epsilon_f' = 0.28$ (28 per cent) pre-anneal and $c = -0.439$ and $\epsilon_f' = 0.22$ (22 per cent) post-anneal. An increase of N_f in the plastic regime may be obtained by increasing ϵ_f' and by decreasing c (lower negative value).

The average low cycle Coffin-Manson plots up to $N_f = 10^4$ for the commercial electrodeposited foils GR 1, GR 2 and GR 3 are shown in Figure 4 and for the

Figure 1
 High strain amplitude fatigue of commercial foils

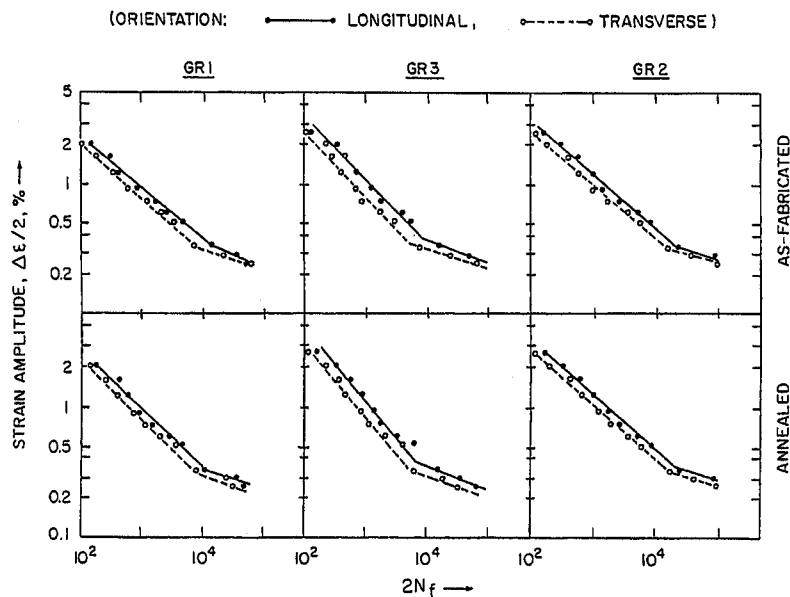
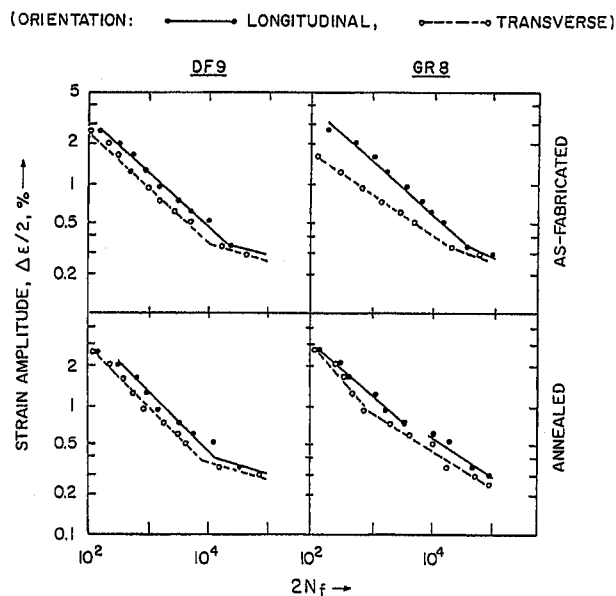


Figure 2
 High strain amplitude fatigue of commercial foils



experimental foils EF, DF 8 and TCAM in Figure 5. The GR 1 foil displays poor fatigue performance; GR 2 and DF 8 show superior N_f over a wide range of $\Delta\epsilon/2$. The latter two foils are compared with the commercial rolled foil GR 8 in Figure 6. Except for the longitudinal orientation in the as-fabricated condition, the DF 8 displays an overall distinctively better low cycle N_f performance.

For the as-fabricated longitudinally oriented GR 8 foil, the boundaries of the pancaked grains provide an effective barrier to the propagation of fatigue crack; upon annealing, this exceptional fatigue life performance falls off owing to: 1 partial recrystallization of the rolled microstructure; and 2 anneal induced embrittlement (Merchant and Clouser, 1996).

Furthermore, the GR 8 foil shows considerable longitudinal versus transverse anisotropy as shown in Figure 7. The anisotropy decreases significantly upon annealing, but would still require a longitudinal sample alignment in order to obtain a good low cycle fatigue performance.

(ii) High cycle fatigue

For $\Delta\epsilon/2 < 0.5$ per cent and $N_f > 10^4$, the results for the commercial foils GR 1, DF 9 and GR 8 and for the experimental foils DF 8 and TCAM are shown in Figures 8 and 9 respectively. In view of the time-consuming nature of the test (high N_f , 1 Hz), a full range of longitudinal results are developed for the (rolled) GR 8 foil; only a few transverse

Figure 3
 High strain amplitude fatigue of experimental foils

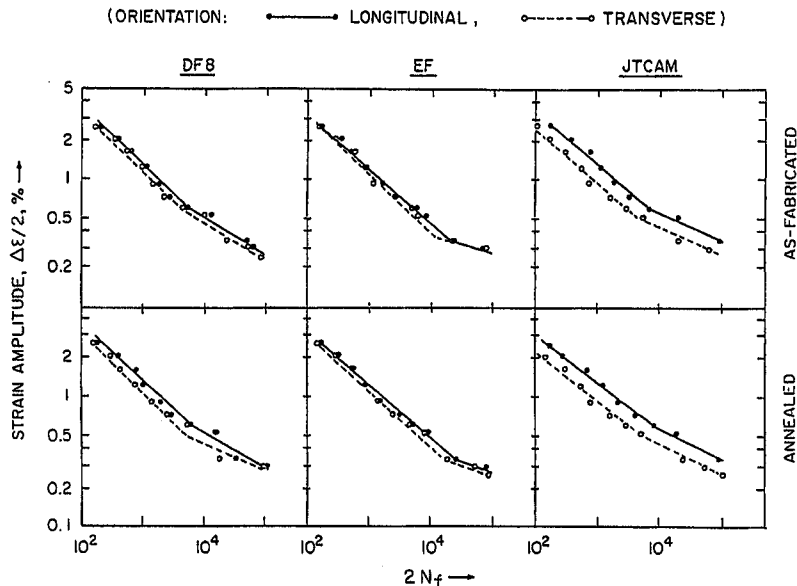
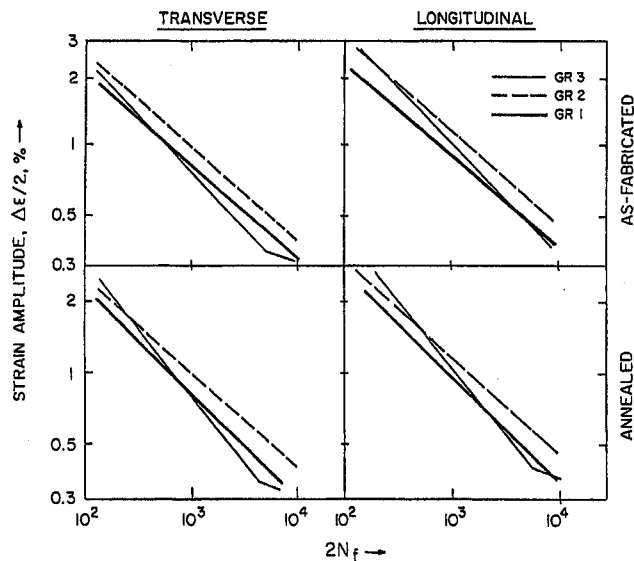


Figure 4
 High strain amplitude fatigue of commercial foils



results are obtained to establish a general trend. For the remaining electrodeposited foils, a full range of transverse results are developed and only a generalized trend for the longitudinal samples.

Except for GR 8 and TCAM, the orientation effect is small and decreases with increasing N_f ; for GR 8 and TCAM, the orientation effect becomes more marked with N_f . For all foils, except for annealed GR 8 and as-fabricated DF 8, relatively small $\log(\Delta\epsilon/2)$ versus $\log(2N_f)$ slope is interrupted by a precipitous slope between $N_f = 10^5$ and 10^6 . This type of change of slope is not uncommon for

fatigue of copper (Pedersen, 1990), but the behavior remains largely unexplained.

Based on the results of Figures 8 and 9, the average high cycle fatigue plots for the electrodeposited foils are shown in Figures 10 and 11. The DF 9 displays a significant improvement in fatigue resistance over the GR 1 (Figure 10). The TCAM is prone to a highly pronounced directional anisotropy upon annealing; by comparison, the post-anneal anisotropy disappears altogether for DF 8 (Figure 11). A comparison of the high cycle fatigue for GR 8 and DF 9 is shown in Figure 12. In the as-fabricated condition, GR 8 is prone to a high directional anisotropy; in the annealed

Harish D. Merchant,
 Melvin G. Minor Jr,
 Sid J. Clouser and
 Dan T. Leonard
 18 μm electrodeposited copper foil
 for flex fatigue applications
 Circuit World
 25/1 [1998] 38-46

Figure 5
 High strain amplitude fatigue of experimental foils

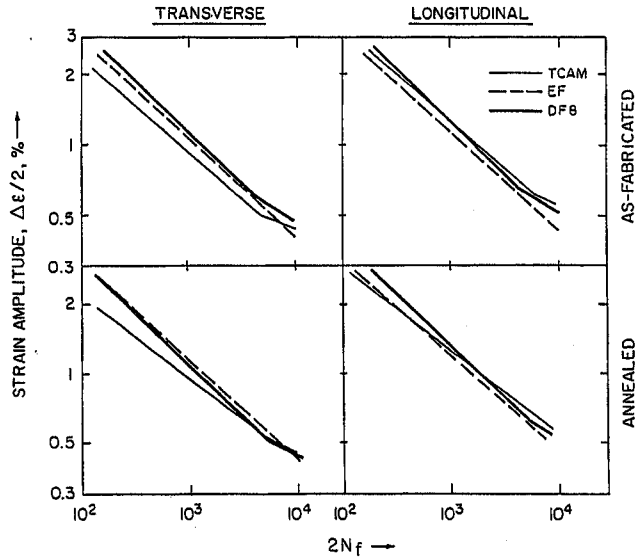
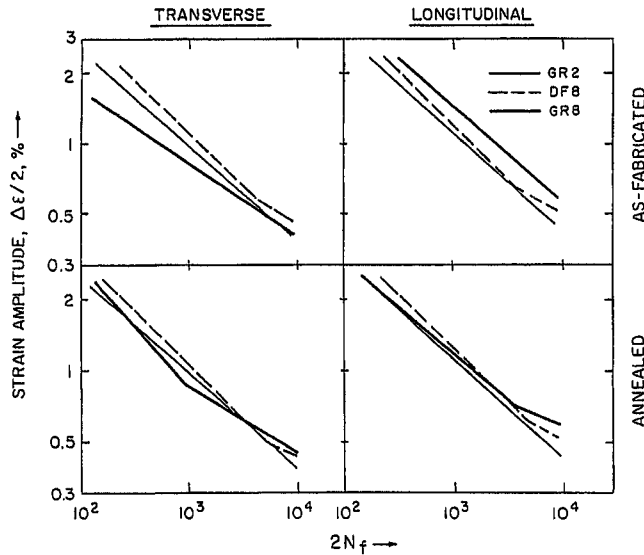


Figure 6
 High strain amplitude fatigue of GR 2, DF 8, and GR 8 foils



condition, this anisotropy decreases and a comparable fatigue behavior is displayed by GR 8 and DF 9.

The parameters σ_f/E , σ_f and b in equation (1) can be determined from the average high cycle fatigue plot immediately following the knee for the plastic to elastic transition: the slope represents b and the intercept at $2N_f = 1$ on the strain amplitude axis represents σ_f/E . Typical values for the annealed DF 8 foil in the transverse orientation are $b = -0.11$, $\sigma_f/E = 2.72 \times 10^{-3}$ and $\sigma_f = 43.52$ ksi (for $E = 12 \times 10^6$ psi). An increase in N_f in the elastic range may be obtained by increasing σ_f (or σ_f/E) and by decreasing b (lower negative value). Note that in this case, σ_f approximately equals the strength σ (see Table 1); hence σ has a direct bearing on N_f .

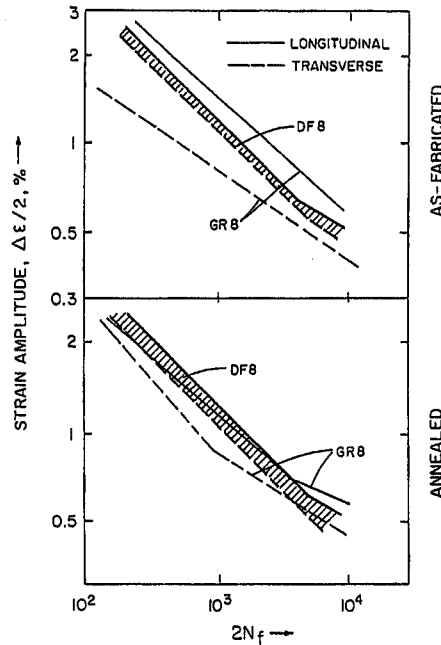
(iii) Fatigue ductility

The strain amplitude can be expressed in terms of the intrinsic material parameter, fatigue ductility D_f^f (Engelmaier and Wagner, 1988):

$$\frac{\Delta \epsilon}{2} = D_f^{0.75} \frac{\sigma}{E} N_f^{-0.6} + 0.9 \left[\exp(D_f^{0.36}) \right]^{0.1785} (10^5/N_f)^{0.1785} \quad (3)$$

Here the first term is plastic component and the second term is elastic component of the strain amplitude; σ is the ultimate tensile strength. An iterative process permits the calculation of D_f , which ought to be independent of $\Delta \epsilon/2$, that is independent of p , t and t_m .

Figure 7
Directional anisotropy of high strain amplitude fatigue of DF 8
and GR 8 foils



The tensile properties of the eight foils are summarized in Table I. Employing $\Delta\epsilon/2$ versus N_f data presented in the previous section. σ from Table I, $E = 12 \times 10^6$ psi for the electrodeposited foils and $E = 16 \times 10^6$ psi for the rolled foil. the calculated D_f for each foil was found to be reasonably constant for N_f between 100 and 1,000. However, beyond that range, but still within the plastic regime for N_f up to about 10^4 , the D_f showed considerable scatter. The calculated D_f values from $\Delta\epsilon/2$ versus N_f data in the elastic regime were too small (electrodeposited foils) or too large (rolled foil) and are clearly invalid.

Confining the D_f calculation for the mandrel sizes 40, 52 and 62 mil ($\Delta\epsilon/2$ between 1 and 2 per cent), credible estimates of D_f were obtained. The average results and scatter band are shown in Figure 13; the scatter is large for

the rolled foil, especially in the annealed condition where the anneal induced embrittlement yields a wide array of D_f values. The foils are ranked in terms of D_f (Figure 13). The experimental DF 8 and EF foils are a vast improvement over the conventional commercial foil GR 1 and they are superior to the rest of the electrodeposited foils. Except for the as-fabricated rolled foil, where the boundaries of pancaked grains offer resistance to the propagation of fatigue cracks, the DF 8 foil has D_f values comparable to those for the GR 8 rolled foil.

(iv) Fatigue ductility and fatigue life

Comparing the plastic components of equations (1) and (2),

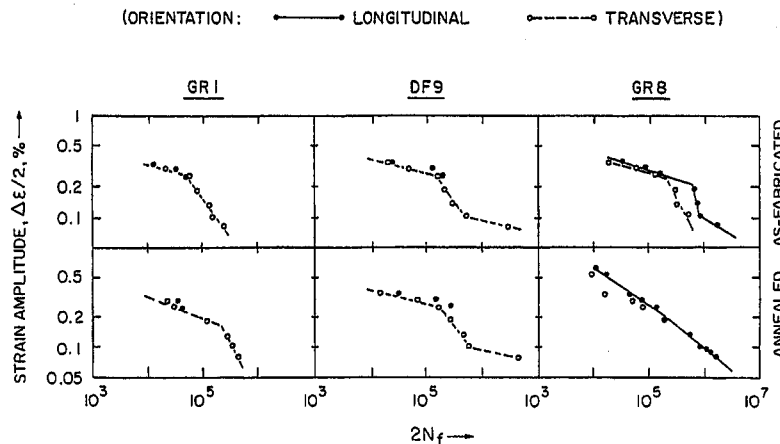
$$D_f = (\epsilon_f')^{1.33}, \quad c = -0.6 \log(N_f) / \log(2N_f) \quad (4)$$

It is immediately clear that the fatigue ductility is a measure of strain accommodation in the low cycle fatigue prior to failure. Given the value of intercept ϵ_f' , it is possible to estimate D_f . For example, ϵ_f' for the longitudinally oriented rolled foil GR 8 is 0.28 pre-anneal and 0.22 post-anneal (Figure 6). Substituting in equation (4), D_f is 84 per cent pre-anneal and 61 per cent post-anneal. These D_f values are close to those obtained from equation (3) by an iterative procedure.

An increase in N_f in the plastic fatigue regime may be obtained by increasing ϵ_f' , that is by increasing D_f . The parameter D_f is intrinsically independent of variations in foil thickness or bend radius which however affect N_f significantly. Given an average N_f for the low cycle fatigue, it is possible to determine the parameter c which is the sensitivity of N_f to the geometrical parameters. For example, average fatigue life for mandrel sizes between 40 and 62 mil for the longitudinally oriented GR 8 in the annealed condition is $N_f^{av} = 181$; substituting in equation (4) yields $c = 0.53$.

D_f is hence an incomplete description of low cycle fatigue resistance; it measures strain accommodation ϵ_f' , but not the sensitivity of N_f to geometrical factors, that is the parameter c . The parameter which bridges D_f to a more pertinent engineering description of low cycle fatigue, N_f , is the foil strength σ . This is illustrated in Figure 14 which shows universal relations D_f^{av} with $N_f^{av}\sigma$ and N_f^{av} with $D_f^{av}\sigma$. All foils in the pre-anneal and post-anneal conditions and in the longitudinal and transverse orientations fit these empirical relationships within a reasonable scatter band. Exceptions are the GR 8 and TCAM foils in longitudinal orientation due to their microstructural propensity to embrittlement (TCAM) or reinforcement (GR 8) or both (post-anneal GR 8).

Figure 8
Low strain amplitude fatigue of commercial foils



Harish D. Merchant,
Melvin G. Minor Jr,
Sid J. Clouser and
Dan T. Leonard
18 μm electrodeposited copper foil
for flex fatigue applications

Circuit World
25/1 [1998] 38-46

Figure 9
Low strain amplitude fatigue of experimental foils

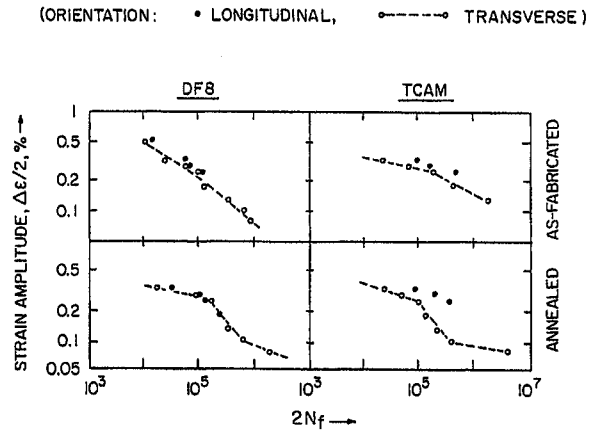


Figure 10
Low strain amplitude fatigue of GR 1 and DF 9 commercial foils

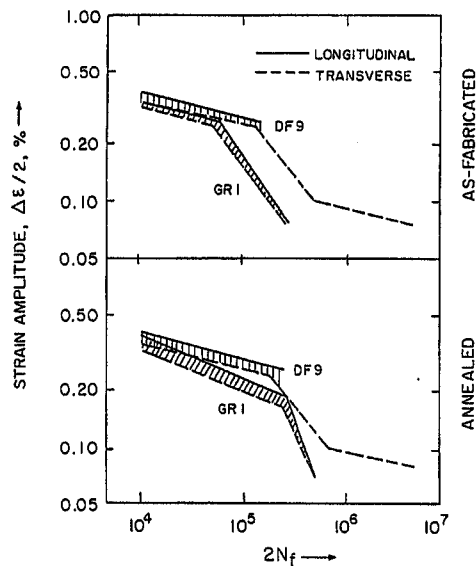


Figure 13 ranks the foils in terms of the low cycle fatigue life parameter $D_f^{0.5} \cdot \sigma$. Again, the electrodeposited foils generally outperform the rolled foil GR 8 except for the longitudinal pre-anneal condition where a specific microstructural fatigue reinforcement apparently occurs.

Discussion

(i) D_f and high cycle fatigue

Comparing the elastic components of equations (1) and (3), it can be shown that

$$b = 1 - \left[\log(2N_f) \right]^{-1} \left[1.29 + \log(\epsilon) D_f \right] - 0.1785 \log N_f \quad (5)$$

Note a small contribution of D_f to b . Although the stresses in the high cycle regime are primarily elastic, the crack propagation and fatigue failure occur by plastic deformation. In other words, the stress concentration around the propagating crack ensures that the local stress level is in

excess of the yield stress. For $D_f = 0.3$ to 1.0 (30 to 100 per cent) and N_f between 10^5 and 10^6 , the calculated $b = -0.1$ using equation (5). The experimental values of b are reasonably close to the calculated value. Decreasing D_f tends to decrease b (see equation (5)) and, hence, to increase the high cycle N_f . At sufficiently high N_f , b approaches zero; as $b \rightarrow 0$, from equation (5), the fatigue limit $N_f^{(C)}$ is defined by

$$\log N_f^{(C)} = 5.602 \left[1.29 + \log(\epsilon) D_f \right] \quad (6)$$

For $D_f = 1$ (100 per cent), $N_f^{(C)} = 10^{9.6}$; for $D_f = 0.1$ (10 per cent), $N_f^{(C)} = 10^{7.5}$. Hence, depending upon the D_f value, a limiting condition ($b = 0$) is predicted for $N_f^{(C)}$ between $10^{7.5}$ and $10^{9.6}$. Note that $N_f^{(C)}$ increases with D_f .

(ii) D_f and tensile properties

For a large class of metals, a first-approximation for strain-life curve is given as (Meyers and Chawla, 1984):

Harish D. Merchant,
 Melvin G. Minor Jr.,
 Sid J. Clouser and
 Dan T. Leonard
 18 μm electrodeposited copper foil
 for flex fatigue applications
 Circuit World
 25/1 [1998] 38-46

Figure 11
 Low strain amplitude fatigue of DF 8 and TCAM experimental foils

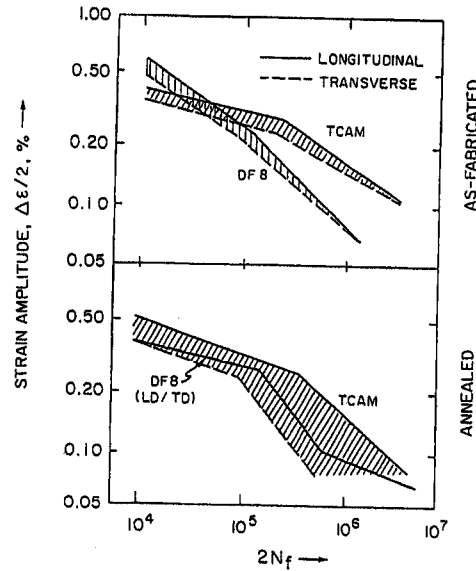


Figure 12
 Low strain amplitude fatigue of GR 8 and DF 9 commercial foils

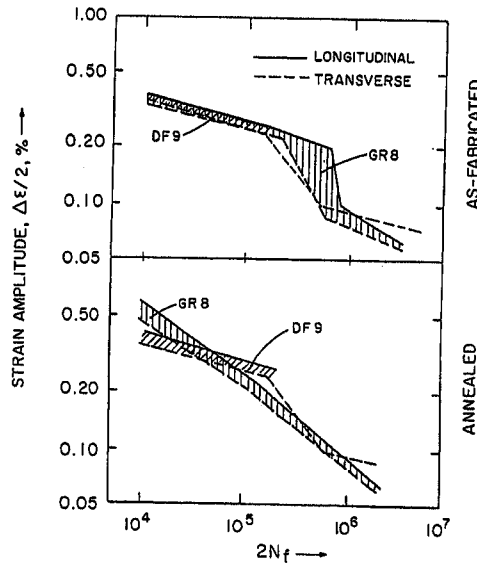


Table I
 Tensile properties* of 18 μm foils

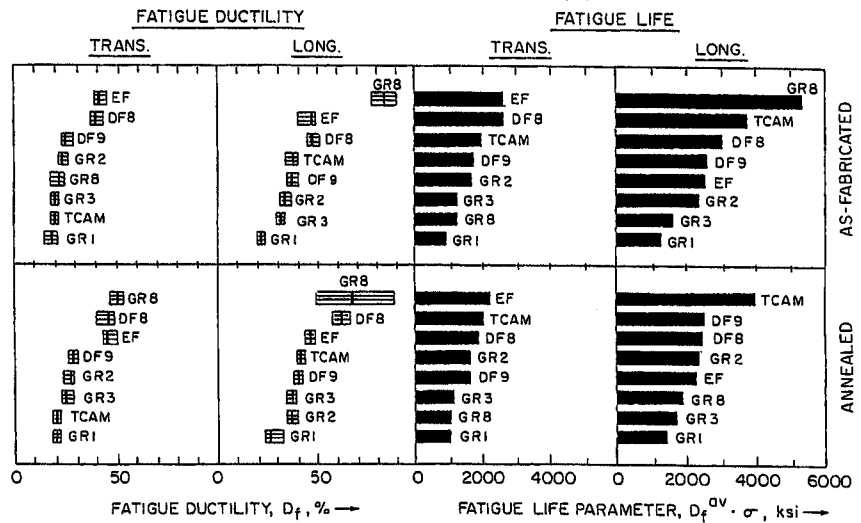
	Strength (KSI)				Peak elongation (%)				Total elongation (%)			
	**AF		ANN		AF		ANN		AF		ANN	
	***L	T	L	T	L	T	L	T	L	T	L	T
GR 1	56	56	54	54	10	11	13	12	18	14	19	16
GR 2	72	72	67	67	3.3	3.4	3.2	3.6	9.9	7.8	8.7	5.8
GR 3	52	51	47	46	13	12	17	17	15	14	18	18
GR 8	65	58	28	23	1.5	0.8	9.8	7.4	1.5	0.9	10	7.5
DF 9	73	72	64	63	3.4	3.7	4.5	4.7	13	11	17	15
DF 8****	67	66	41	40	6.8	7.4	24	22	10	10	25	23
EF****	55	55	52	52	13	12	14	15	19	17	20	19
TCAM****	102	100	96	95	3.5	3.4	3.2	3.0	7.7	3.9	3.5	3.1

Notes: *23°C, 2in/min crosshead speed; **AF = as fabricated; ANN = annealed, 225°C, ten minutes; ***orientation: L = longitudinal; T = transverse; ****experimental foils

Harish D. Merchant,
Melvin G. Minor Jr.,
Sid J. Clouser and
Dan T. Leonard
18 μm electrodeposited copper foil
for flex fatigue applications

Circuit World
25/1 [1998] 38-46

Figure 13
Fatigue ductility (D_f) and fatigue life (N_f) rankings for 18 μm commercial and experimental foils



$$\Delta \epsilon = 3.5 (\sigma/E) N_f^{-0.12} + \epsilon_f^{0.6} N_f^{-0.6} \quad (7)$$

where ϵ_f is true strain at fracture in tension. If A_0 and A_f are the initial area and the cross-sectional area in the fracture region respectively and $q = 1 - (A/A_0)$ is reduction of area, $\epsilon_f = \ln(A/A_0) = \ln[(1-q)^{-1}]$ represents the maximum true strain that the material can withstand before fracture. A comparison of equations (1) and (7) indicates that $D_f \approx \epsilon_f^{0.8}$.

Since the strain calculated from the engineering strain (elongation) is not valid beyond the onset of necking, it is not possible to calculate (or to relate to) ϵ_f from elongation. For the GR 3, GR 8, DF 8 and TCAM foils, the post-anneal peak and total elongations are identical (Table I), hence, no necking occurs during tensile test. Here the elongation should be indicative of ϵ_f . There is, however, no correlation between the post-anneal elongation values for these foils and the corresponding D_f values (Figure 13). In order to dispel the occasionally held notion that the tensile elongation is somehow related to D_f , the peak and total elongations for all foils are plotted against D_f in Figure 15. Absence of correlation between elongation and fatigue ductility is apparent.

As a general rule, ductile materials give the best performance for the low cycle fatigue conditions while strong and low modulus (high σ/E) materials give the best results for the high cycle fatigue conditions (Reed-Hill and Abbaschian, 1992; Smallman, 1985). However, much caution should be exercised in invoking this generality for thin foils. Except for the fact that in low cycle fatigue the strength provides an empirical bridge between D_f and N_f (Figure 14), no correlation exists between tensile strength or elongation and fatigue performance.

(iii) Strain hardening

During fatigue, an initially hard and strong metal usually softens and an initially soft metal usually hardens (Meyers and Chawla, 1984). The cyclic hardening or softening occurs during the first 100 or so cycles; after which an equilibrium value of strain hardening parameter n' , defined by $\Delta \sigma = K' (\Delta \epsilon_p)^{n'}$ where $K' = \sigma_f / (\epsilon_f)^{n'}$ (Courtney, 1990), is operative. Adding the elastic and plastic components of strain, the cyclic stress-strain curve is given as (Dowling, 1978)

$$\Delta \epsilon = \Delta \sigma / E + (\Delta \sigma / K')^{1/n'} \quad (8)$$

The cyclic strain hardening is inherent to the metal and is related to the corresponding strain hardening parameter n in

the tensile loading. When $n > 0.15$ or σ / σ_y (σ_y is yield strength and σ is ultimate strength) > 1.4 , cyclic hardening is predicted; when $n < 1.5$ and $\sigma / \sigma_y < 1.2$, cyclic softening may occur (Reed-Hill and Abbaschian, 1992).

The parameters b and c in equation (1) are related to n (Meyers and Chawla, 1984):

$$b = -n' / (1 + 5n'), \quad c = -1 / (1 + 5n'), \quad b/c = n' \quad (9)$$

Figure 14
Universal correlations of fatigue ductility (D_f) and fatigue life (N_f) with tensile strength (σ)

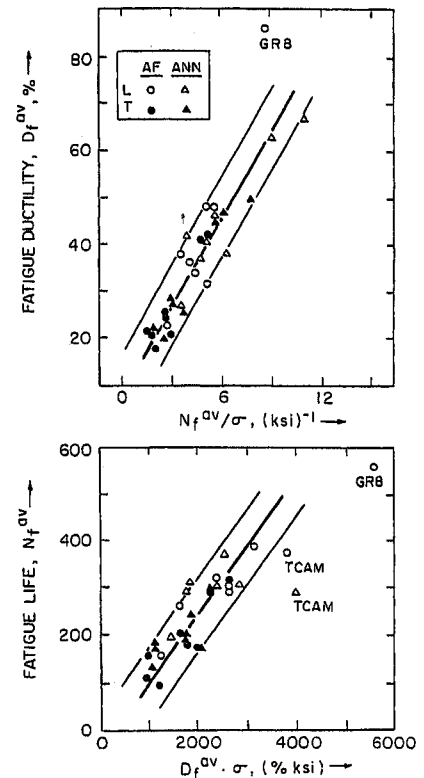
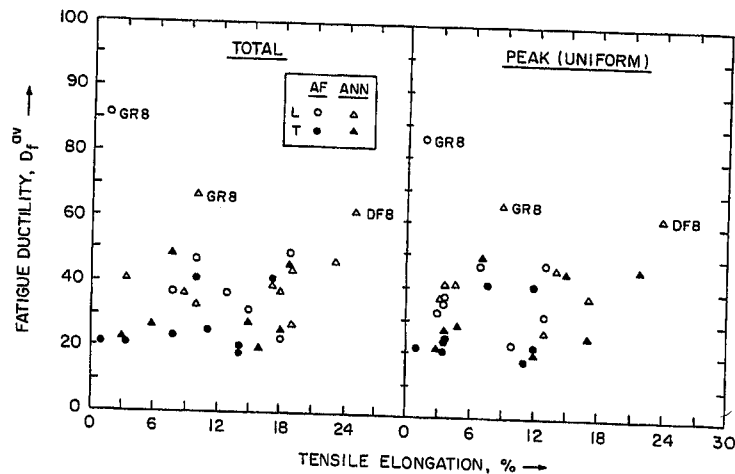


Figure 15
Correlation between fatigue ductility (D_f) and tensile elongation



For metals, n' typically lies between 0.1 and 0.3 which relates to $n = 0.2$ obtained in monotonic tensile test. Both c and b decrease with increasing n' and hence N_f in the low as well as the high cycle fatigue is enhanced for a high n' foil.

Typical calculated n' (in cyclic loading) for the pre-anneal and post-anneal DF 8 foil is 0.27; the corresponding experimental values of n (in monotonic loading) are 0.20 pre-anneal and 0.17 post-anneal, suggesting significantly higher hardening rates in the cyclic loading. For the (rolled) GR 8 foil, the calculated n' pre-anneal is 0.33, but after dead-soft (225°C, ten minutes) anneal it becomes 0.14. Accordingly, the pre-anneal GR 8 is prone to soften during fatigue, but in the post-anneal condition it shows considerable cyclic hardening; as has been shown recently by the microhardness measurements of fatigued samples (Merchant *et al.*, 1997).

Conclusions

- 1 The flex fatigue performance of 18 μm electrodeposited foil, in the low cycle (DF 8 foil) and the high cycle (DF 9 foil) regimes, equivalent to that of the 18 μm rolled (GR 8) foil has been demonstrated. The rolled foil is prone to an anneal induced loss of fatigue resistance and a highly directional fatigue response (fatigue anisotropy). The DF 8 and DF 9 foils show an enhancement of fatigue resistance following an anneal exposure and the fatigue behavior that is largely non-specific to direction with respect to the foil surface roll markings.
- 2 The fatigue life (N_f) is an essential engineering parameter which depends sensitively on geometrical factors such as foil thickness and bend radius during fatigue; both in turn depend upon the strain amplitude per cycle ($\Delta\epsilon/2$). The fatigue ductility (D_f) is an intrinsic low cycle fatigue material parameter which is independent of the geometrical factors. N_f and D_f together describe the fatigue behavior. For all foils, N_f is universally related to the strength (σ) weighted D_f . The N_f and D_f rankings of seven electrodeposited foils and the rolled foil are provided.
- 3 For each foil and either (low cycle and high cycle) fatigue regime, N_f is inversely related to D_f as the Coffin-Manson (C-M) relationship. The C-M parameters (b , c , ϵ_f and σ_f/E) uniquely describe the

fatigue performance: (i) N_f is enhanced by increasing ϵ_f and σ_f/E and by decreasing b and c . (ii) D_f is directly related to ϵ_f . (iii) σ_f is an approximate measure of metal strength (σ), and (iv) b and c together correspond to the cyclic strain hardening parameter (n').

- 4 Except for the fact that σ bridges the fatigue parameters D_f and N_f in the form of an empirical universal relationship valid for all foils, the tensile properties of the foil do not accurately reflect its fatigue performance.

References

- Courtney, T.H. (1990). *Mechanical Behavior of Materials*. McGraw-Hill, New York, NY, pp. 562-624.
- Dowling, N.E. (1978). "Stress-strain analysis of cyclic plastic bending and torsion". *J. Eng. Materials Tech.*, Vol. 100, pp. 157-63.
- Dowling, N.E. (1993). *Mechanical Behavior of Materials*. Prentice-Hall, Englewood Cliffs, NJ, pp. 621-71.
- Engelmaier, W. (1987). "Results of the IPC copper foil ductility round-robin study". in *Testing of Metallic and Inorganic Coatings*. STP 947. ASTM, pp. 66-95.
- Engelmaier, W. and Wagner, A. (1988). "Fatigue behavior and ductility determination for rolled annealed copper foil and flex circuits on Kapton". *Circuit World*, Vol. 4 No. 2, pp. 30-8.
- Merchant, H.D. and Clouser, S.J. (1996). "Effect of thermal exposure on flex and fold fatigue performance of fine grained electrodeposited copper foil". *IPC National Conf. on Flex Circuits*. Bedford, MA.
- Merchant, H.D., Clouser, S.J. and Minor, M.G. (1996). "Fold fatigue performance of 18 μm copper foil". *FLEXCON '96*. Sunnyvale, CA.
- Merchant, H.D., Minor, M.G. and Rozboril, M.G. (1997). "Characterization of damage during flex fatigue of 18 μm copper foil". *IPC National Conf. on Flex Circuits*. Phoenix, AZ.
- Meyers, M.A. and Chawla, K.K. (1984). *Mechanical Metallurgy: Principles and Applications*. Prentice-Hall, Englewood Cliffs, NJ, pp. 688-731.
- Pedersen, O.B. (1990). "Mechanism maps for cyclic plasticity and fatigue of single phase materials". *Acta Metall. Mater.*, Vol. 38 No. 7, pp. 1221-39.
- Reed-Hill, R.E. and Abbaschian, R. (1992). *Physical Metallurgy Principles*. PWS-Kent, Boston, MA, pp. 755-71.
- Smallman, R.E. (1985). *Physical Metallurgy*. Butterworth-Heinemann, Stoneham, MA, pp. 463-74.